Original Article
Targeting β2 subunit of Na+/K+-ATPase induces glioblastoma cell apoptosis through elevation of intracellular Ca2+

Shirong Li[1,2*], Zhi Dai[1*], Dong Yang[1*], Wenxuan Li[3], Hongjuan Dai[1], Bin Sun[1], Xiuyun Liu[1,2], Xin Xie[4], Rong Xu[5], Xudong Zhao[1,6,7]

[1]Key Laboratory of Animal Models and Human Disease Mechanisms of Chinese Academy of Sciences and Yunnan Province, Kunming Institute of Zoology, Chinese Academy of Sciences/Key Laboratory of Bioactive Peptides of Yunnan Province, Kunming 650223, Yunnan, China; [2]Kunming College of Life Science, University of Chinese Academy of Sciences, Kunming 650204, Yunnan, China; [3]College of Life Sciences, Sichuan University, Chengdu 610064, Sichuan, China; [4]Stake Key Laboratory of Drug Research, The National Center for Drug Screening, Shanghai Institute of Materia Medica, Chinese Academy of Sciences, Shanghai 201203, China; [5]Department of Neurosurgery, Huashan Hospital, Fudan University, Shanghai 200040, China; [6]CAS Center for Excellence in Animal Evolution and Genetics, Chinese Academy of Sciences, Kunming 650223, China; [7]Kunming Key Laboratory of Healthy Aging Molecular Mechanism Study, Kunming 650223, Yunnan, China. *Co-first authors.

Abstract: Glioblastoma (GBM) is the most frequent brain cancer with poor prognosis and few therapies and urgently requires effective treatments. Na+/K+-ATPase is considered as a target for GBM therapy and development of anticancer drugs. Cardiac glycosides bind the Na+/K+-ATPase α subunit to inhibit enzymatic activity and are promising candidates for anticancer drug development including GBM. However, the comparatively higher doses required for effective anticancer actions cause severe cardiotoxicity. Selectively targeting the ATPase Na+/K+ transporting subunit beta 2 (ATP1B2) that is not expressed in the heart might avoid the cardiotoxicity. However, the effect of targeting ATP1B2 in GBM remains unknown. In this study, we found that high ATP1B2 expression is significantly associated with poor prognosis of patients with GBM. ATP1B2 silencing in GBM cells resulted in remarkably cell cycle arrest at the G2/M phase and apoptosis with concomitant increase in intracellular Ca2+ and activation of p38 kinase, similar to Na+/K+-ATPase inhibition by the classic cardiac glycoside digoxin. ATP1B2 is expressed higher in glioblastoma stem-like cells (GSCs) than in GBM cells and its downregulation induces apoptosis of GSCs. Furthermore, inducible ATP1B2 knockdown significantly inhibit tumor growth *in vivo*. Our data suggest ATP1B2 has potential as a therapeutic target for GBM.

Keywords: ATP1B2, Na+/K+-ATPase, glioblastoma, digoxin

Introduction

Na+/K+-ATPase is a ubiquitously expressed membrane protein complex that maintains the ionic homeostasis or electrochemical gradient of cells [1]. In addition to its actions as an ion pump, Na+/K+-ATPase also functions as a signaling scaffold, participating in cell signaling events involving cell-cell interactions, proliferation, and apoptosis [2, 3]. Studies have clarified the involvement of aberrant expression and activity of Na+/K+-ATPase in tumorigenesis and tumor progression. Changes in Na+/K+-ATPase subunit expression have been characterized in various cancers [4, 5], including glioblastoma (GBM) [6, 7]. Na+/K+-ATPase has emerged as a powerful therapeutic target for glioblastoma therapy. GBM is ranked as the most common and aggressive type of brain cancer with median survival of < 15 months [8], and further elucidation of its mechanisms and drug development is a priority.

Na+/K+-ATPases are composed of distinct isoforms of α and β subunits [9], some of which contain additional γ subunits [10]. Cardiac glycosides, which have emerged as a promising therapeutic candidates for cancer [11], are known to be specific inhibitors of Na+/K+-ATPase [12] where they bind to the alpha sub-

unit to inhibit enzymatic activity [13]. Some cardiac glycosides or derivatives have been tested in phase I and II clinical trials to treat cancers [14-16]. Currently, 16 clinical trials of the classic cardiac glycoside digoxin are listed on the website of National Institutes of Health (NIH, https://clinicaltrials.gov/ct2/results?cond=cancer&term=digoxin). Several preclinical research studies have reported the anti-GBM activity of cardiac glycoside [17, 18]. By binding to Na$^+$/K$^+$-ATPase, cardiac glycosides activate a series of downstream signaling cascades to induce GBM cell apoptosis [7]. These facts further strongly suggest that the Na$^+$/K$^+$-ATPase enzyme could be an important target for GBM therapy and Na$^+$/K$^+$-ATPase inhibitors could be developed to combat GBM [19].

Although cardiac glycosides have been clinically approved for heart failure for over 200 years, the comparatively higher effective anticancer doses cause arrhythmias [20-22]. Some genes encoding Na$^+$/K$^+$-ATPase subunits are selectively expressed in various tissues [10], providing opportunities to target tissue specific Na$^+$/K$^+$-ATPase without disturbing heart function. The ATPase Na$^+$/K$^+$ transporting subunit beta 2 (ATP1B2) that encodes the Na$^+$/K$^+$-ATPase β2-subunit is selectively expressed in the brain and rarely in the heart muscle and other tissues [9, 23]. The β2-subunit (ATP1B2) was initially identified as the adhesion molecule on glial cells (AMOG), which mediates astrocyte adhesion and migration [24] and ATP1B2 loss promotes invasion of GBM [25].

The β-subunit is a glycoprotein involved in the structural and functional maturation of Na$^+$/K$^+$-ATPase, and it regulates the enzyme stability, alpha subunit activity, and cell adhesion processes [26]. We hypothesized that targeting ATP1B2 might induce cytotoxicity on GBM cells similar to that induced by cardiac glycosides. In this study, we found that ATP1B2 silencing induced cellular apoptosis and inhibited tumor growth. Furthermore, the expression of ATP1B2 is reversely correlated to disease prognosis.

Materials and methods

Cell culture

U87 and T98G GBM cells were cultured in Dulbecco's modified Eagle's medium (DMEM) supplemented with 10% fetal bovine serum (FBS, Millipore, USA), 100 U/mL penicillin and 100 mg/mL streptomycin (Life Technologies, USA). U87 and T98G cell lines were authenticated using Short Tandem Repeat (STR) profiling.

U87 and T98G GBM stem-like cells (GSCs) were enriched as previously reported [27]. Briefly, U87 and T98G cell lines stably expressing doxycycline-inducible shATP1B2-1# were seeded in six-well plates containing GBM stem-like cell medium, DMEM F12 (Gibco, USA) with 1 × B27 (Life Technologies, USA), 50 ng/mL epidermal growth factor (EGF, Peprotech, USA) and basic fibroblast growth factor (bFGF) (Peprotech, USA). After suspended tumor spheres were visible using microscopy, they were passaged and cultured in DMEMF12 to enrich the GSCs. The cells collected after six passages were used for experiments. The GSCs marker Nestin and SOX2 were detected using real-time quantitative polymerase chain reaction (qPCR) and flow cytometry.

RNA extraction and real-time qPCR

Total RNA was extracted using the PureLink™ RNA mini kit (Life Technologies, USA) according to the manufacturer's protocol. DNA was removed using a DNA-free™ kit (Invitrogen, USA). Total RNA was reversed transcribed using random primers with a cDNA synthesis kit (Thermo Scientific, USA). The qPCR was performed using the SYBR Green method (Life Technologies, USA) and normalized to the level of 18S rRNA. Primers are shown in Supplementary Table 1.

Cell proliferation assay

5-Bromo-2'-deoxyuridine (BrdU) or 5-ethynyl-2'-deoxyuridine (EdU, 10 µM each) was added to the cell medium and incubated for 1 h. For BrdU staining, cells were fixed with 4% paraformaldehyde, permeabilized with 0.3% Triton-100, treated with 2 M hydrochloric acid (HCl) for 30 min, and blocked with 10% goat serum for 1 h. The cells were incubated with the primary anti-BrdU antibody (Abcam, UK) for 1 h, followed by the CY3-labeled secondary antibody (Life Technologies, USA). EdU staining was performed according to the manufacturer's protocol (Invitrogen, USA).

Soft agar colony formation assay

Cells were suspended in medium with 0.4% agarose (Sigma-Aldrich, USA) and then plated into six-well plates containing bottom gel (0.8% agarose). On the second day, doxycycline (dox) was added to medium at a final concentration of 1 μg/mL to knockdown ATP1B2, and the medium was refreshed every 3 days. At the end of the experiments, 4% formaldehyde containing 0.005% crystal violet was added to fix and stain the colonies, the images were acquired using a digital camera, and then the colonies were counted.

Western blot analysis

Cells were washed with cold phosphate-buffered saline (PBS) and lysed with radioimmunoprecipitation assay (RIPA) lysis buffer (50 mM Tris-HCl, 150 mM sodium chloride, 1% IGEPAL CA-630 [Sigma-Aldrich, USA], 0.1% sodium dodecyl sulfate [SDS]), 0.5% sodium deoxycholate, and 0.1 mg/mL phenylmethylsulfonyl fluoride [PMSF, Sigma-Aldrich, USA] plus 1 × phosphatase and protease inhibitor [Roche, Switzerland] on ice. The protein concentration was determined using a standard BCA assay kit (Beyotime, China). Equal amounts of total protein were separated using standard SDS-polyacrylamide gel electrophoresis (PAGE). The membranes were then incubated 4°C overnight with anti-p38, anti-phospho-p38 (both Cell Signaling Technology, USA), and anti-β-actin (ProteinTech, USA) antibodies diluted in 5% bovine serum albumin (BSA). The bands were detected using horseradish peroxidase (HRP)-conjugated secondary antibodies and the enhanced chemiluminescence (ECL) reagent according to the manufacturer's protocol (Millipore, USA).

Histological analysis and immunohistochemistry

Formalin-fixed, paraffin-embedded samples were detected using conventional hematoxylin and eosin (H&E) staining according to a standard manufacturer's protocol. For immunohistochemical staining, 5-μm-thick sections were deparaffinized, processed for antigen retrieval, blocked with 10% goat serum, and incubated with primary antibodies against anti-ATP1B2 (Novus Biologicals, USA), antiKi-67 (Vector Laboratories, USA), and anti-cleaved caspase-3 (Cell Signaling Technology, USA) at 4°C over-

night. This was followed by incubation with Cy3, DyLight 488-labeled or HRP-conjugated secondary antibodies to label the primary antibodies. The tissue microarray was bought from Shanghai chengke biotechnology Co., Ltd.

Immunofluorescence staining

Cells cultured on coverslips were fixed with 4% paraformaldehyde, permeabilized with 0.3% Triton-100, and blocked with 10% goat serum for 1 h. Then, the cells were incubated with the primary antibodies (anti-α-tubulin [Sigma-Aldrich, USA]) followed by CY3- or DyLight 488-labeled secondary antibody. DNA was stained with 4,6-diamidino-2-phenylinodole (DAPI).

Lentiviral preparation and infection

The validated target sequences ([Supplementary Table 2](#)) of ATP1B2 short hairpin RNA (shRNA) were from Sigma-Aldrich (https://www.sigmaaldrich.com/catalog/genes/ATP1B2?lang=zh&region=CN#shRNA%20Products) and were cloned into a pLKO.1-stuffer or Tet-pLKO-puro vector (Addgene) according to the manufacturer's protocol. The cDNA encoding human ATP1B2 were amplified from the cDNA of U87 and were mutated to not targeted for degradation by sh-1# and cloned into a HA-tagged plasmid. HEK293T cells were co-transfected with the lentiviral plasmids, packaging plasmids pCMVΔ8.9 and pMD2.G at a ratio of 10:5:2. The cultured supernatant containing the lentiviral particle was separated by ultracentrifugation. The lentivirus was resuspended in PBS with 0.1% BSA and stored at -80°C. The lentiviral particles were titrated by qPCR and the GBM cell lines were infected at a multiplicity of infection (MOI) of 100.

Xenograft mouse models

Six-week-old BALB/c nude mice were purchased from Vital River Laboratory Animal Technology Co., Ltd. (Beijing, China). For subcutaneous xenograft models, $1 × 10^6$ U87 cells stably infected with a doxycycline-inducible ATP1B2 shRNA-1# were mixed with 30% Matrigel (BD Biosciences, USA) and injected subcutaneously into each nude mouse. The mice were divided into two groups on day 7, which were treated as follows: the control group received 5% sucrose while experimental group was administered 2 mg/mL doxycycline plus 5% sucrose. Appro-

ximately 4 weeks later, the mice were euthanized, the tumors were excised, fixed in formalin, and embedded in paraffin. The animal experiment was approved by the animal ethics committee of the Kunming Institute of Zoology, Chinese Academy of Sciences.

Apoptosis, cell cycle, intracellular Ca^{2+} ([Ca^{2+}]i) levels, mitochondrial membrane potential (MMP) and ATP levels detection

To detect apoptosis, cells were trypsinized, resuspended in 200 μL buffer, incubated with 5 μL Annexin V-fluorescein isothiocyanate (FITC) for 10 min, and then 10 μL propidium iodide (PI, eBioscience, USA). The cells were analyzed using flow cytometry (BD, USA). For cell cycle evaluation, cells were trypsinized, fixed in 70% ethanol at 4°C overnight, washed twice in PBS, and then incubated with a solution containing PI and RNase (each 0.02 mg/mL, Sigma-Aldrich, USA) at 37°C for 30 min in the dark. The cell cycle was analyzed using flow cytometry. To detect intracellular Ca^{2+} ([Ca^{2+}]i) levels, cells were incubated with 1 μM Fluo-3-AM (Beyotime, China), a [Ca^{2+}]i indicator, for 1 h at 37°C in a cell incubator. Cells were then trypsinized, resuspended in 200 μL PBS, and analyzed using flow cytometry. MMP were detected by using 5,5',6,6'-tetrachloro-1,1',3,3'-tetraethyl-imidacarbocyanine iodide (JC-1) assay kit (Beyotime, China) according to the manufacturer's protocol. ATP levels were determined according to the manufacture's instruction (ATP Assay Kit, S2006B, Beyotime, China).

Survival curve

The survival curves were analyzed using the Kaplan-Meier survival method and log-rank tests, using the data of 153 patients with GBM who were divided into two groups, with the higher quartile expression of the ATP1B2 as the cut-off level. All the overall survival data and ATP1B2 RNA sequencing (RNA-seq) expression data were obtained from The Cancer Genome Atlas network.

Results

High ATP1B2 expression is associated with poor prognosis in patients with GBM

Protein and RNA expression data from the Human Protein Atlas (HPA) database shows that ATP1B2 subunit is selectively expressed in the brain (**Figure 1A** and Supplementary Figure 1A), with very low expression in heart muscle and other tissues (https://www.proteinatlas.org/ENSG00000129244-ATP1B2/tissue). We also confirmed that ATP1B2 mRNA levels in the mouse brain are much higher than those in the heart using qPCR (Supplementary Figure 1B). Among various types of cancers, ATP1B2 is expressed exclusively in GBM (Supplementary Figure 1C, https://www.proteinatlas.org/ENSG00000129244-ATP1B2/pathology). To determine the expression of ATP1B2 in patients with GBM, we applied immunohistochemistry on a tissue microarray containing 17 pairs of GBM and adjacent non-tumor tissues. ATP1B2 expression was elevated significantly in eight of 17 pairs GBM tissues compared to adjacent non-tumor tissues (**Figure 1B**).

We then investigated the clinical relevance of the relationship between ATP1B2 expression and survival of patients with GBM. The records of the 153 patients with GBM with both data on RNA-seq of ATP1B2 expression and survival were from The Cancer Genome Atlas (TCGA). The Kaplan-Meier survival curve showed that the quartile patients with high ATP1B2 expression had worse overall survival (**Figure 1C**, P = 0.0074). These results demonstrated that ATP1B2 is a predictor of survival of patients with GBM, which implies that ATP1B2 may play important roles in GBM development and progression.

ATP1B2 knockdown inhibits GBM cells proliferation and induces cell cycle arrest similar to digoxin

To explore the role of ATP1B2 in GBM, U87 and T98G cells were infected with ATP1B2 shRNAs or negative control (shCtr) lentivirus. ATP1B2 expression was downregulated efficiently by shRNA-1# and shRNA-2# (Supplementary Figure 2A and 2B). Approximately 4 days after infection, there were less cells in the ATP1B2 silenced group than there were in the control group. The BrdU and EdU proliferation assays revealed that ATP1B2 knockdown significantly decreased the proliferation of both cell lines (**Figure 2A** and **2C**) compared to that of the negative control, and the Na$^+$/K$^+$-ATPase inhibitor digoxin also inhibited GBM cell proliferation (**Figure 2B** and **2D**).

We examined whether ATP1B2 silencing impairs the cell cycle, and its downregulation elevated the G2/M cell population of U87 and
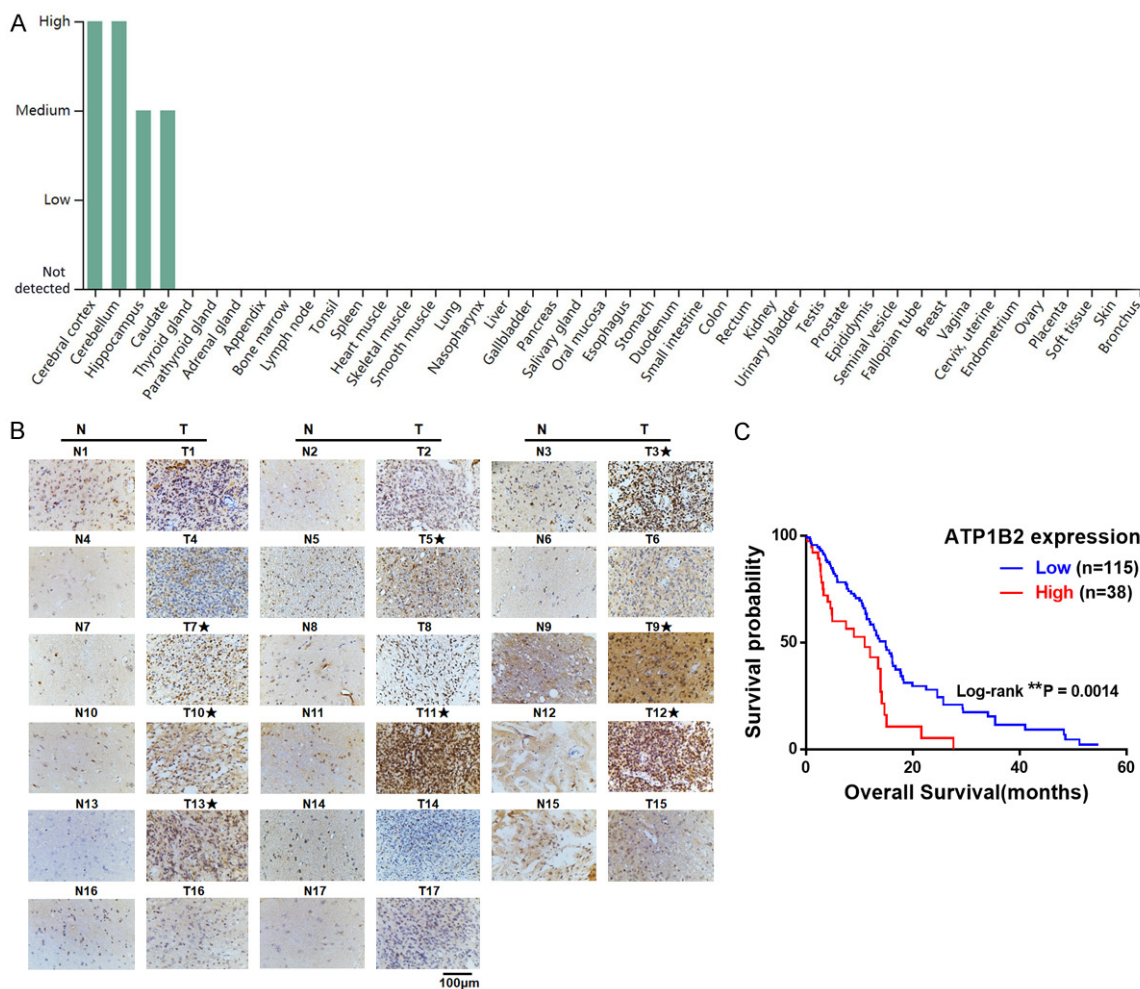
Figure 1. High ATP1B2 expression is associated with poor prognosis in patients with glioblastoma (GBM). A. ATP1B2 protein expression levels of human tissues from Human Protein Atlas (HPA). B. Immunohistochemical staining for ATP1B2 in GBM tissues (T) and in adjacent non-tumor tissues (N). The GBM tissues with significantly elevated ATP1B2 expression are labeled by asterisks. C. Kaplan-Meier survival analysis of overall survival in TCGA of patients with GBM with ATP1B2 high or low levels, *, P < 0.05.

T98G cells accompanied by the decrease of cell population at the G1 phase (**Figure 2E** and **2G**). This observation suggested that the cell cycle was arrested at the G2/M phase. We also verified that pharmacological inhibition of Na$^+$/K$^+$-ATPase using digoxin resulted in similar effects on U87 and T98G cells (**Figure 2F** and **2H**). Taken together, these data indicated that inhibition by ATP1B2 and digoxin induced similar cell-cycle arrest.

ATP1B2 downregulation induces apoptosis and inhibits GBM colony formation in vitro

The phenotype of ATP1B2 knockdown in U87 and T98G cells was observed for a longer ti-

me, downregulation of ATP1B2 leads to swelling of U87 and T98G cells, formation of vacuole, shrinkage of pseudopod and progressively destroyed (Supplementary Figure 3), since ATP1B2 is known as an adhesion molecule, previous studies indicated repletion of the β subunit resulted in abundant stress fibers [28] and inhibition of Na$^+$/K$^+$-ATPase prevented the formation of bundled stress fibers [29]. Immunofluorescence staining of β-actin and α-tubulin indicated stress fibers were less evident and the cell cytoskeleton were destroyed after ATP1B2 knockdown (**Figure 3A**). Finally, cells exhibited apoptotic characteristics: rounding and shrinking, Annexin V-FITC/PI double-staining using flow cytometry was used
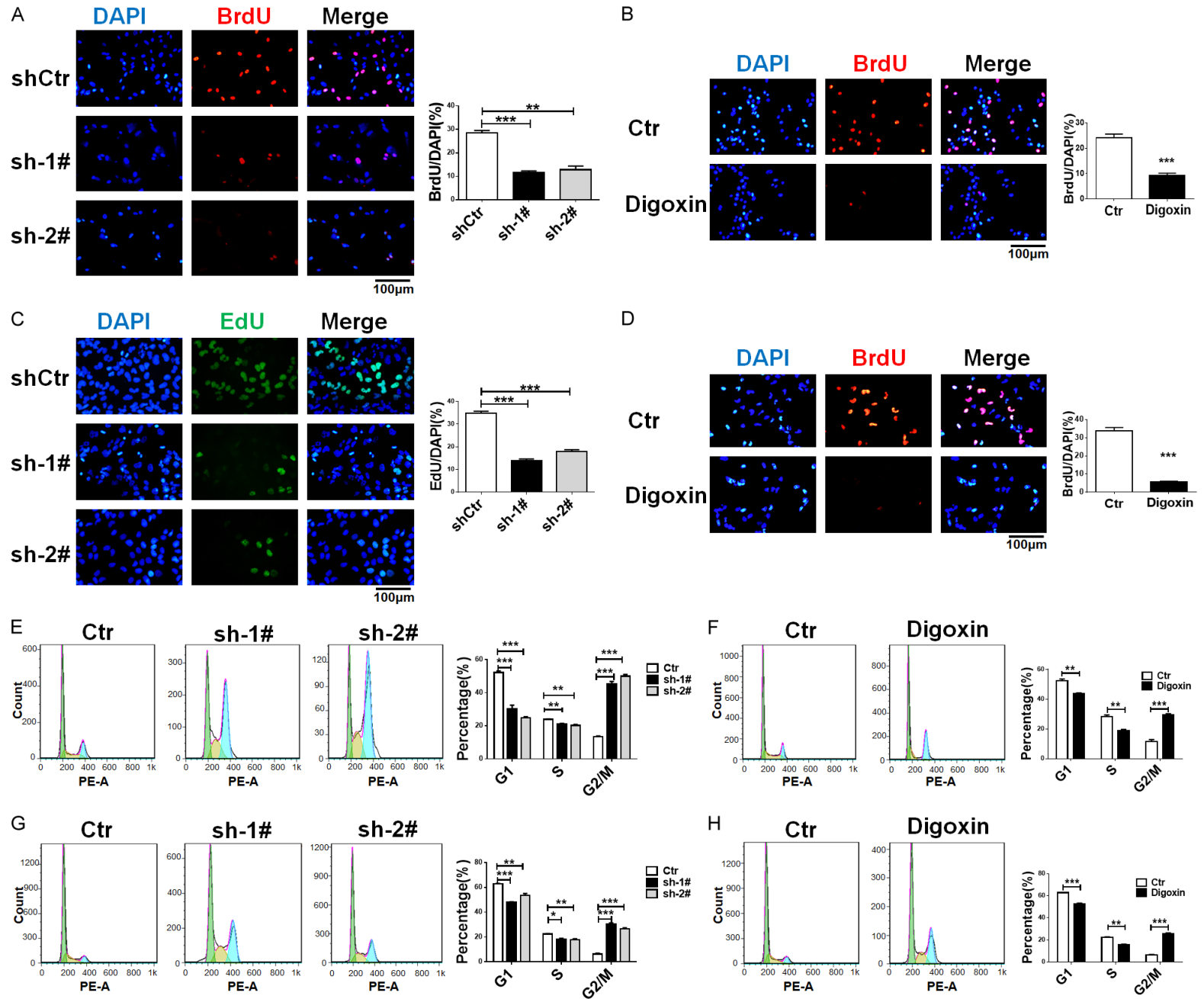
Figure 2. ATP1B2 knockdown inhibits GBM cells proliferation and cell cycle arrest similar to digoxin. (A-D) 5-Bromo-2'-deoxyuridine (BrdU) or 5-ethynyl-2'-deoxyuridine (EdU) incorporation assay was used to evaluate proliferation rates of ATP1B2 downregulation and digoxin treatment of (A, B) U87 and (C, D) T98G. Quantifications are shown at the right. Data are means ± SD, *, P < 0.05 and ***, P < 0.001. (E-H) Cell cycle analysis of ATP1B2 downregulation and digoxin treatment of (E, F) U87 and (G, H) T98G cells stained with propidium iodide (PI) and DNA content measured using flow cytometry. Quantifications are shown at the right. Data are means ± SD, *, P < 0.05 and ***, P < 0.001.

identify apoptosis. Compared with the control groups, both shATP1B2-1# and 2# induced a significantly higher percentage of apoptotic cells. Additionally, digoxin also induced apoptosis of the GBM cell lines (**Figure 3B**).

Long-term soft agar colony assays were used to assess the colony-forming capacity of GBM cells following ATP1B2 knockdown. U87 and T98G cells were engineered to express inducible shATP1B2-1# to downregulate ATP1B2 expression following doxycycline induction. This doxycycline-inducible shRNA significantly reduced ATP1B2 mRNA levels in U87 and T98G cells (Supplementary Figure 2C). Compared to the control, doxycycline-induced ATP1B2 knockdown substantially reduced the colony numbers and size (**Figure 3C** and **3E**). Furthermore, digoxin also similarly inhibited the U87 and T98G cell lines (**Figure 3D** and **3F**).

ATP1B2 is highly-expressed in GSCs and its downregulation induces apoptosis of GSCs

When exposed to doxycycline, U87 and T98G cell lines that stably expressed shATP1B2-1# were also induced to apoptosis (**Figure 4A** and **4B**). A previous study reported that ATP1B2 is highly expressed in GSCs [25]. We enriched GSCs derived from U87 and T98G cell lines that stably expressed shATP1B2-1# following doxycycline induction. The success of GSCs enrichment was confirmed by the expression Nestin and SOX2, GSC markers. Compared with U87 and T98G cells, immunofluorescence staining using flow cytometry showed upregulation of ATP1B2 and the GSC marker Nestin in U87-GSC and T98G-GSC (**Figure 4C** and **4D**). The qPCR also confirmed that ATP1B2 as well as Nestin and SOX2 were upregulated in the enriched GSCs (Supplementary Figure 4A and 4B). Furthermore, doxycycline-induced ATP1B2 silencing (Supplementary Figure 4C and 4D) also induced GSC death. Annexin V-FITC/PI double-staining indicated that ATP1B2 downregulation induced significant U87-GSC and T98G-GSC apoptosis (**Figure 4E** and **4F**). These

results confirmed that ATP1B2 suppression induced apoptosis of both GBM cells and GSCs.

ATP1B2 downregulation increases [Ca^{2+}]i levels and activates p38 mitogen-activated protein kinase (MAPK) pathway

The proapoptotic effects of cardiac glycosides have been connected sustained elevation of [Ca^{2+}]i [30]. To gain insight into the mechanisms by which ATP1B2 knockdown induces apoptosis, we investigated whether its repression influenced [Ca^{2+}]i levels. The cytosolic calcium levels were examined using flow cytometry with the [Ca^{2+}]i indicator, Fluo-3-AM probe. The fluorescence intensity significantly increased after ATP1B2 suppression in U87 and T98G cells. Similarly, U87 and T98G cells treated with digoxin showed a marked increase in [Ca^{2+}]i levels (**Figure 5A**).

Elevated [Ca^{2+}]i levels are known to be an important factor leading to the activation of mitogen-activated protein kinase (MAPK) pathways in human cancers [31], therefore, we determined if p38 MAPK activation was induced by ATP1B2 knockdown. Western blot analysis showed that phosphorylated p38 (p-p38) was significantly increased while little change in total p38 protein was observed (**Figure 5B**). U87 and T98G cells treated with digoxin at the indicated time periods also exhibited robust phosphorylation of p38 (**Figure 5B**). The results suggest that ATP1B2 repression and digoxin activated p38 MAPK. To further supporting the effect of ATP1B2 knockdown on p38 activation, U87 and T98G cells were infected with control vector or a HA-tagged ATP1B2 vector that was mutated to not targeted for degradation by sh-1#, the restoring ATP1B2 expression downregulated the activation of p38 in U87 and T98G (Supplementary Figure 5A). Previous study indicated that inhibition of Na$^+$/K$^+$-ATPase decreased intracellular ATP in glioma cells [32], our results showed that ATP1B2 downregulation and digoxin reduced cellular ATP level in U87 and T98G cells (**Figure**
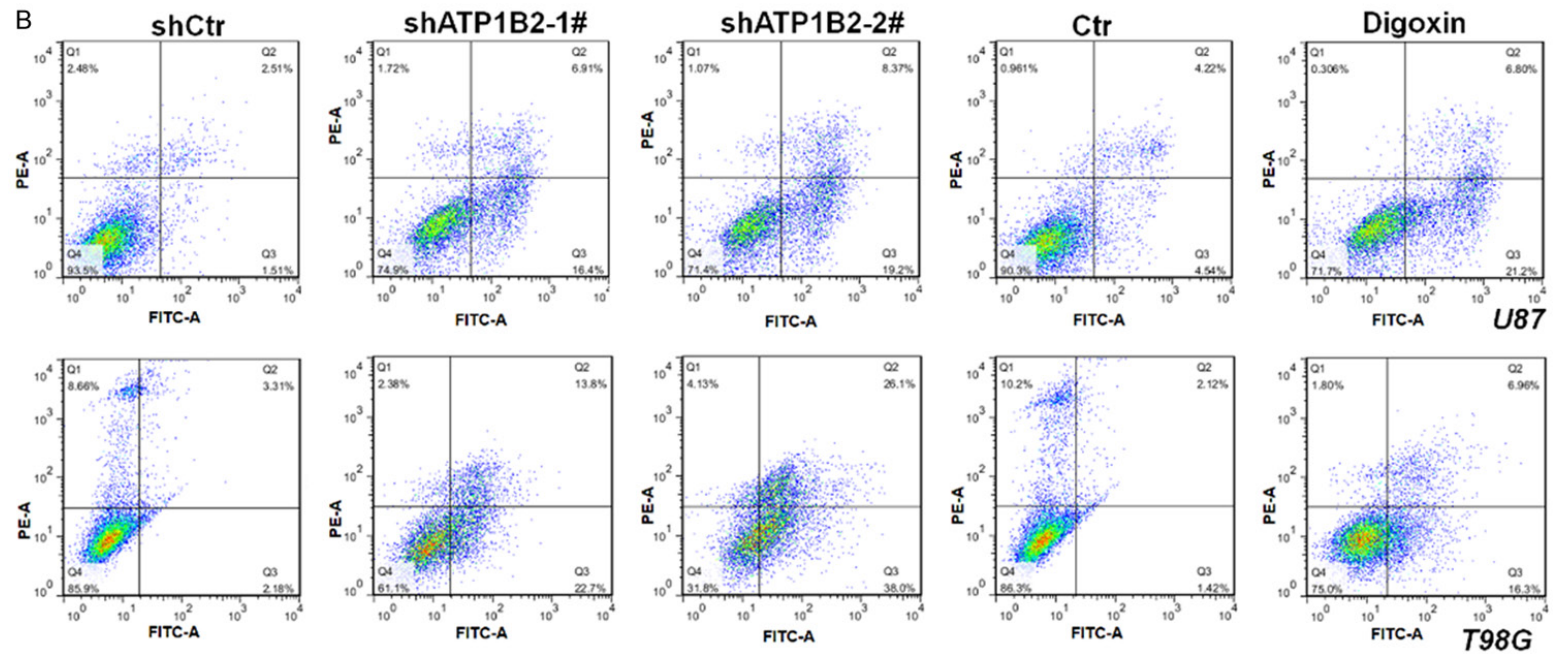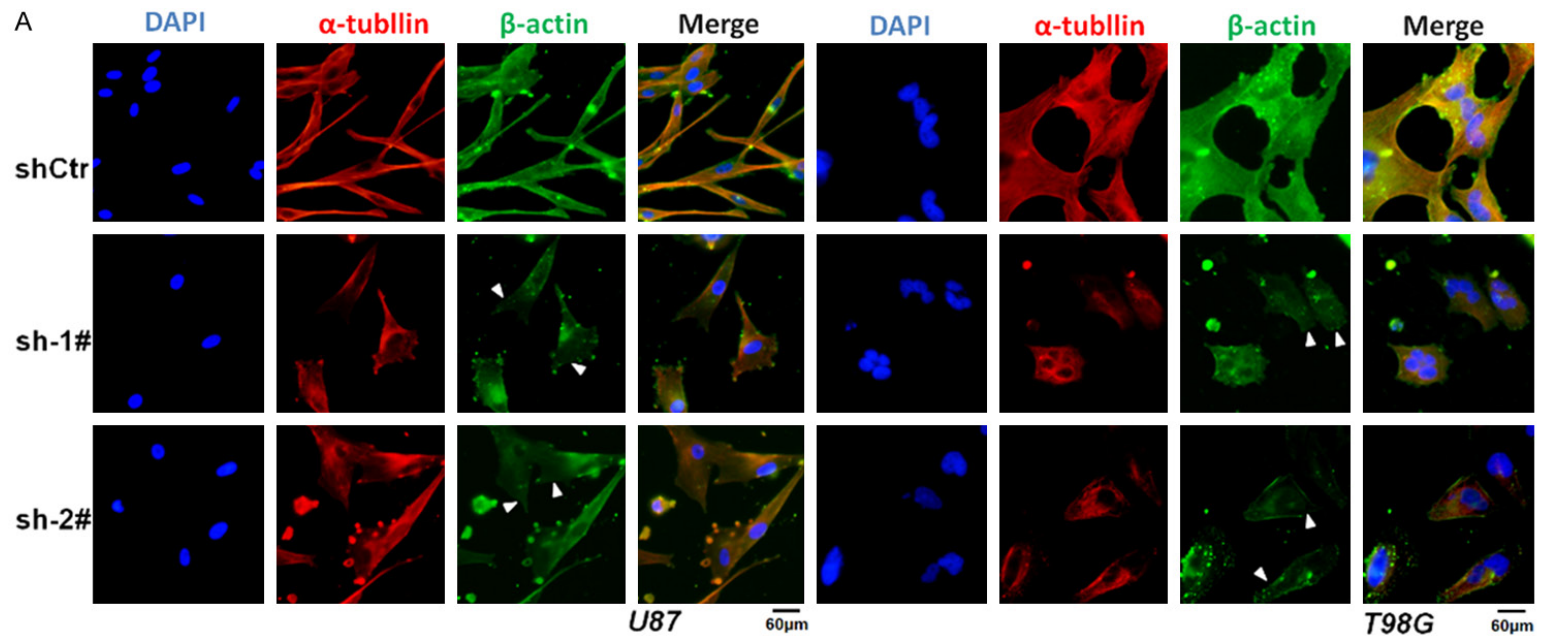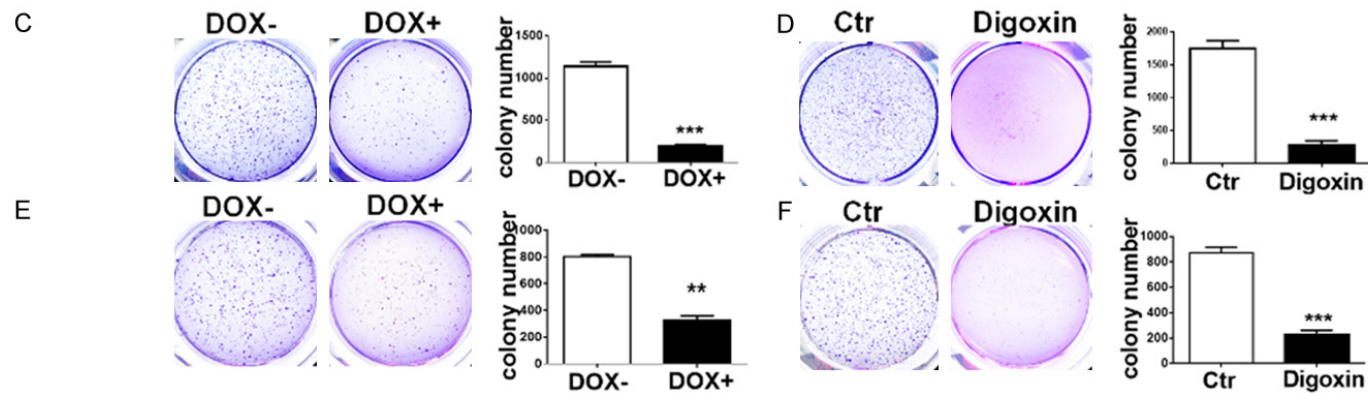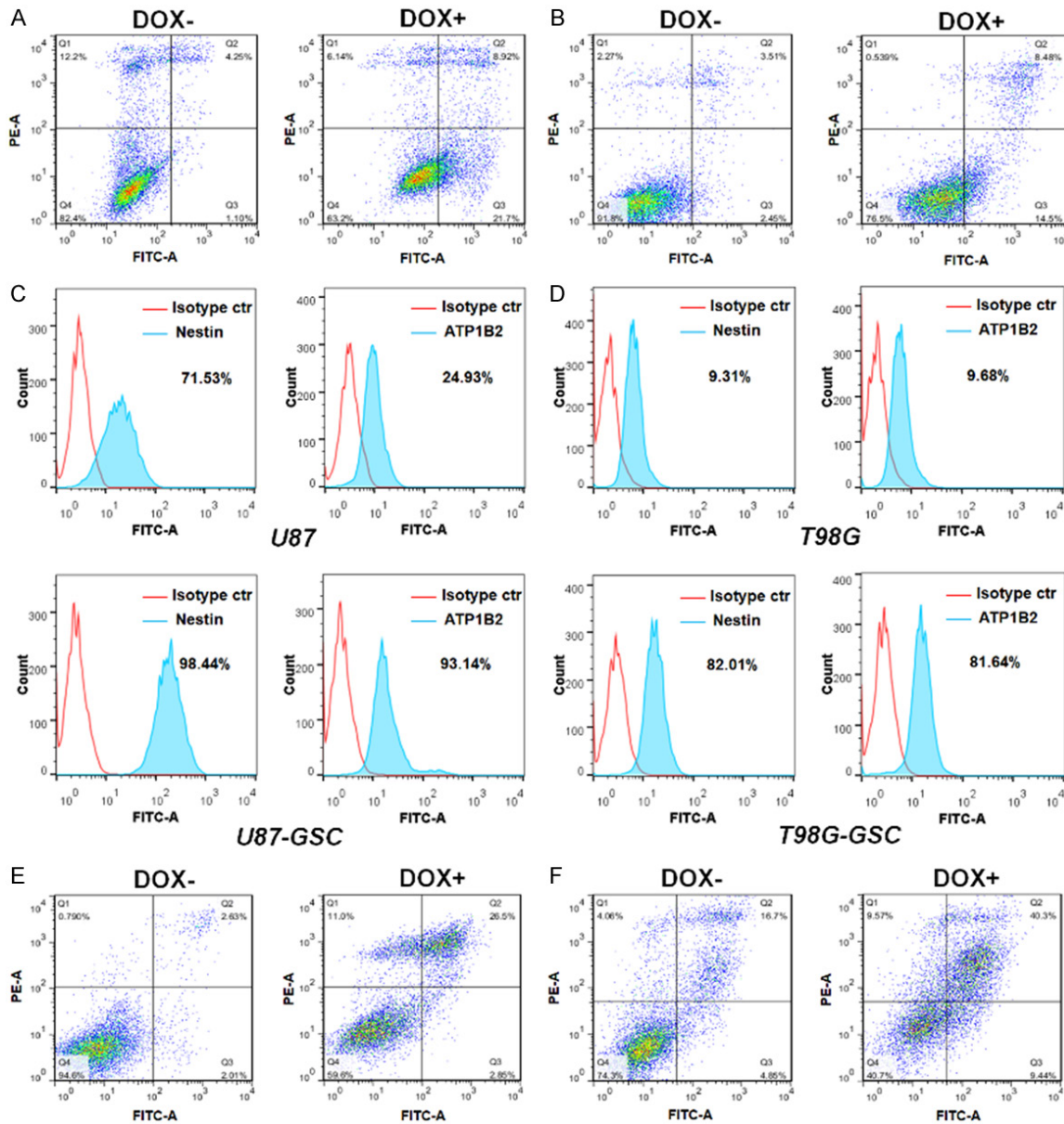
Figure 3. ATP1B2 downregulation induces apoptosis and inhibits GBM cells colony formation *in vitro*. (A) Immunofluorescence staining of β-actin and α-tubulin after ATP1B2 downregulation in U87 and T98G cells, triangles indicate stress fibers were less evident. (B) Annexin V-fluorescein isothiocyanate (FITC)/propidium iodide (PI) double-staining assays for ATP1B2 downregulation and digoxin treatment on apoptosis using flow cytometry of U87 and T98G. (C-F) Soft agar colony formation assay of ATP1B2 downregulation upon doxycycline (DOX) induction and digoxin treatment of (C, D) U87 and (E, F) T98G cells and colonies were stained with crystal violet, photographed, and counted. Quantifications of colonies are shown at the right. Data are means ± SD, *, P < 0.05 and ***, P < 0.001.

Figure 4. ATP1B2 is highly-expressed in glioblastoma stem-like cells (GSCs) and its downregulation induces apoptosis of GSCs. (A, B) Annexin V-fluorescein isothiocyanate (FITC)/PI double-staining assays for dox-induced ATP1B2 downregulation on apoptosis using flow cytometry in (A) U87 and (B) T98G. (C, D) Immunofluorescence staining of ATP1B2 and Nestin expression levels in GSCs enriched from (C) U87 and (D) T98G cells and detected using flow cytometry. The percentage of positive cells are shown in the histogram. (E, F) Annexin V-fluorescein isothiocyanate (FITC)/PI double-staining assays for dox-induced ATP1B2 downregulation on apoptosis using flow cytometry in (E) U87-GSC and (F) T98G-GSC.

5C). The fluorescent probe JC-1, which is a mitochondrial membrane potential (MMP) indicator, showed a loss of JC-1 aggregates after downregulation of ATP1B2 and digoxin treatment (**Figure 5D** and **5E**). Thus, the data indicated that the MMP was disturbed during ATP1B2 suppression induced apoptosis. Furthermore, caspase-3 activation is an integral step in most apoptotic processes, there was a marked increase in activated caspase-3 (**Figure 5F-I**)-positive cells using immunofluorescence with a cleaved caspase-3 specific antibody. Na$^+$/K$^+$-ATPase β subunit is obligatory for function of enzymes, which protects α subunit from cellular degradation [33] and plays a role in the transport of α subunit to the cell surface [26].
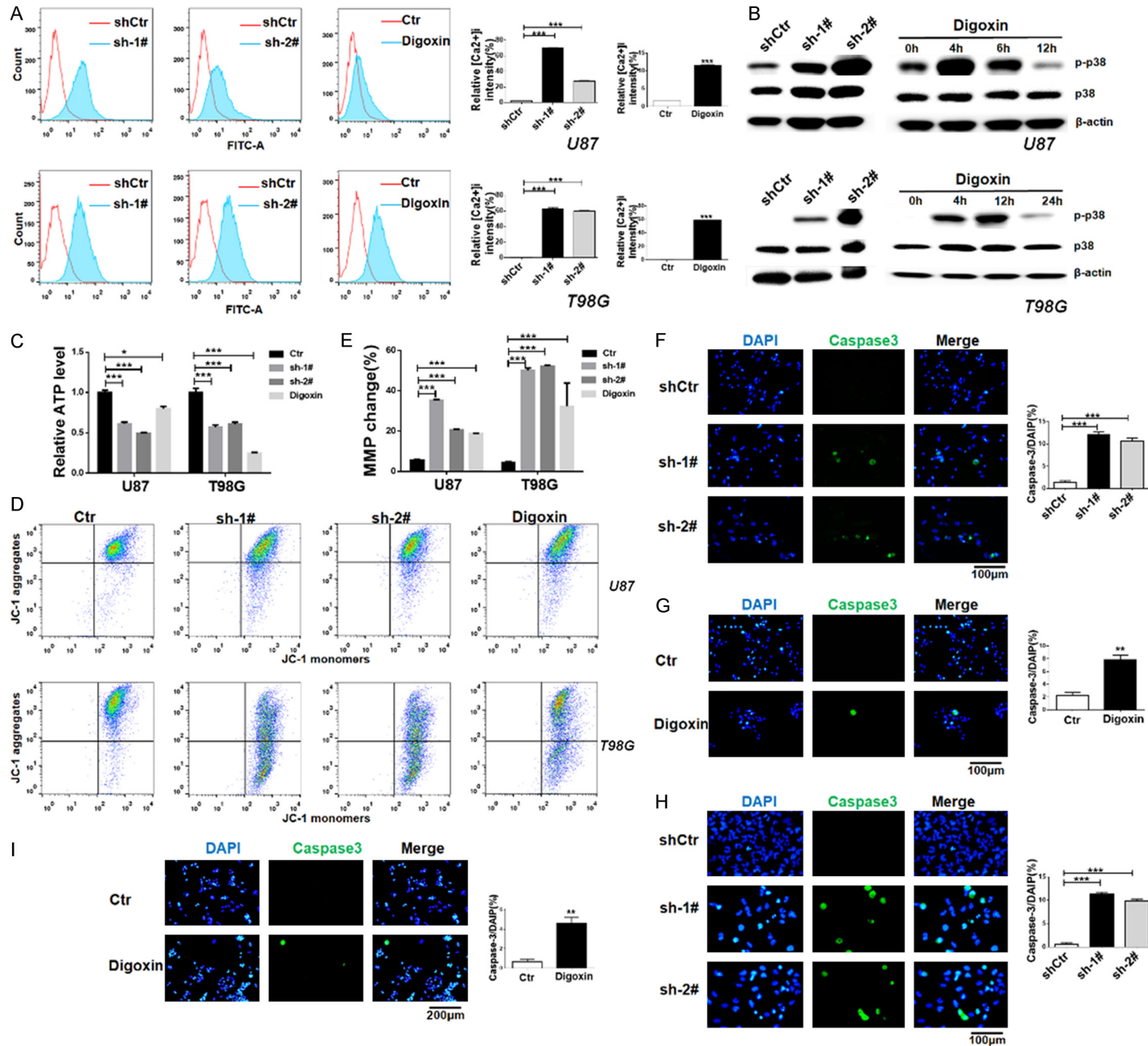
Figure 5. ATP1B2 downregulation increases intracellular calcium ([Ca^{2+}]) levels and activates p38 mitogen-activated protein kinase (MAPK) pathway. (A) [Ca^{2+}]i concentration was quantified using the calcium indicator Fluo-3AM using flow cytometry. U87 and T98G cells were infected with short-hairpin control (shCtr) or shATP1B2-1# and 2# and treated with digoxin. Quantifications are shown at the right. Data are means ± SD, *, P < 0.05 and ***, P < 0.001. (B) Phosphorylated-p38 (p-p38) kinase and total p38kinase were detected using western blotting using specific antibodies. β-actin was the loading control. U87 and T98G cells were infected with shCtr or shATP1B2-1# and 2# and treated with digoxin at indicated times. (C) Cellular ATP levels in U87 and T98G cells after ATP1B2 downregulation and digoxin treatment. Values represent relative mean ATP levels ± SD (*, P < 0.05, ***, P < 0.001). (D, E) Mitochondrial membrane potential (MMP) was quantified by JC-1 using flow cytometry (D). (E) Quantifications are shown at upper panel. Data are means ± SD, *, P < 0.05 and ***, P < 0.001. (F-I) Activation of caspase-3 was detected using specific antibody for cleaved-caspase3 using immunofluorescence after ATP1B2 downregulation and digoxin treatment of (F, G) U87 and (H, I) T98G cells. Quantifications are shown at the right. Data are means ± SD, *, P < 0.05 and ***, P < 0.001.

Na$^+$/K$^+$-ATPase α1 subunit is also required for export of β2 subunit from the endoplasmic reticulum [34]. Upon ATP1B2 knockdown, the qPCR showed that α1 subunit encoded by ATP1A1 was not significantly reduced at mRNA level, but the protein level of ATP1A1 was decreased (Supplementary Figure 5B and 5C). These further support ATP1B2 as an important therapeutic target of Na$^+$/K$^+$-ATPase for GBM.

ATP1B2 repression inhibits GBM growth in vivo

We explored whether ATP1B2 expression is required for *in vivo* tumor growth in mice xenografted with the highly tumorigenic U87 GBM cell line stably expressing doxycycline-inducible shATP1B2-1#. One week later, the mice were separated into two groups, doxycycline was administered to one of the groups (**Figure 6A**). The xenograft growth rates were significantly inhibited in mice administered doxycycline, whereas the control group showed rapid tumor growth (**Figure 6B**). On day 45, the mice were euthanized and tumor volume measurement strikingly revealed that tumor growth in the doxycycline-treated groups was slight. This result indicates that doxycycline-induced ATP1B2 silencing suppressed the tumor volume by 10-fold versus that of the control mice (**Figure 6C** and **6D**), and clearly inhibited tumor growth *in vivo*.

Explanted tumors were also evaluated and repression of ATP1B2 *in vivo* was confirmed using immunohistochemical analysis (**Figure 6E**). Tumors of doxycycline-treated mice showed fewer neoplastic cells in the H&E staining (**Figure 6F**). The cellular proliferation marker Ki-67 was decreased robustly in ATP1B2-suppressed tumors (**Figure 6G**). We also observed significantly more cleaved-caspase-3-positive cells in ATP1B2-silenced tissues

(**Figure 6H**). These observations are consistent with the phenotype of ATP1B2 knockdown *in vitro*. Taken together, these results indicate that ATP1B2 is strongly associated with GBM growth *in vivo* and confirm ATP1B2 as an important potential therapeutic target for GBM.

Discussion

Na$^+$/K$^+$-ATPase is considered an important proof-of-concept target for GBM therapy and development of anticancer drugs [22]. Digoxin as clinically approved cardiac drug has been widely used for heart failure. It specifically binds Na$^+$/K$^+$-ATPase α-subunit to inhibit Na$^+$/K$^+$-ATPase, which is now being explored in several clinical trials for cancer treatment. However, the inherent cardiotoxicity limits its implication in cancer therapy. Na$^+$/K$^+$-ATPase is mainly consisting of α subunits and β subunits. Selectively targeting the Na$^+$/K$^+$-ATPase subunits that are not expressed in the heart might avoid the cardiotoxicity [22]. The β-subunit is also an important part of Na$^+$/K$^+$-ATPase and while current studies have primarily focused on the α subunits, few have investigated the β subunits. A previous study indicated that the β3 subunit (ATP1B3) is overexpressed in gastric cancer, and its downregulation induced significant cancer cell apoptosis [35]. Therefore, the ATP1B3 of Na$^+$/K$^+$-ATPase participates in the tumorigenesis of gastric cancer.

ATP1B2 is recognized as a membrane glycoprotein mediating neuron-astrocyte adhesion and neuronal migration [24]. Later it was identified to form a functional ion pump with α subunit of Na$^+$/K$^+$-ATPase [36]. The previous study identified the involvement of ATP1B2 in glioma invasion and migration [25]. The role of ATP1B2 in GBM remains unclear. In our study, the cell proliferation assay showed that ATP1B2 shRNA-1#
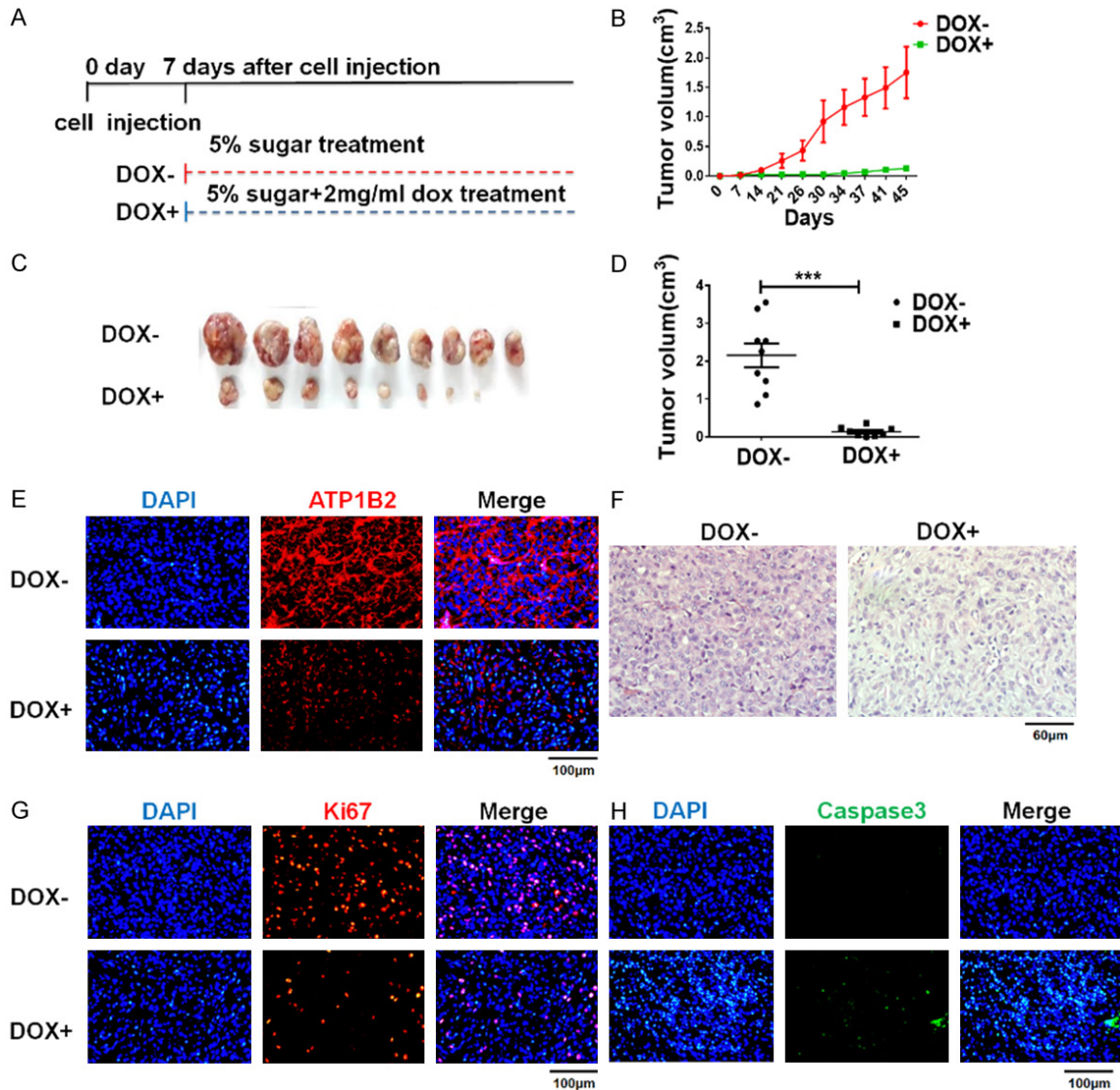
Figure 6. ATP1B2 knockdown inhibits GBM growth *in vivo*. (A) Diagram of BALB/c nude mice were injected with U87 cells stably expressing doxycycline-inducible shATP1B2-1#. DOX- group: mice were administered 5% sugar in water. DOX+ group: mice were treated with 5% sugar plus 2 mg/mL doxycycline. (B) Tumor sizes were measured and shown at right. Results are mean volumes ± SD. (C, D) Tumors from nude mice (C) and tumor volumes are shown at right (D). Each dot represents tumor volume of each mouse. Results are mean volumes ± SD in group, ***, P < 0.001. (E-H) Hematoxylin and eosin (H&E) staining of DOX- and DOX+ group (F). Tumor histology of (E) ATP1B2, (G) Ki67, and (H) cleaved caspase-3 immunohistochemical staining of tumors from DOX- and DOX+ group mice.

and shRNA-2# effectively inhibited the cell proliferation rate of both U87 and T98G cell lines. Similar to digoxin treatment, ATP1B2 knockdown also resulted in G2/M phase arrest and increased apoptosis. Furthermore, downregulation of ATP1B2 inhibited colony formation similar to digoxin. These results suggest that ATP1B2 might be a potential target for GBM treatment, based on its similar anticancer effect to that of digoxin *in vitro*. The concept of ATP1B2 as a potential therapeutic target in

GBM was further supported by the *in vivo* evidence that tumor growth was remarkably inhibited by ATP1B2 downregulation.

The immunohistochemical evaluation indicated ATP1B2 expression was elevated in eight of 17 pairs GBM tissues compared to adjacent non-tumor tissues. We then investigated the clinical survival correlation of ATP1B2 expression in patients with GBM in TCGA. We observed a significant association between high ATP1B2

expression and a dramatic decrease in clinical survival. Patients with higher quartile expression of the ATP1B2 showed shorter overall survival time. These results suggest that ATP1B2 may be a predictor of survival of patients with GBM in clinical research. A previous study identified higher ATP1B2 expression in GSCs than in GBM cells [25]. GSC is a major factor of relapse and therapeutic resistance with poor prognosis, and it is not completely removed by surgery. In our study, the enriched GSCs of both U87 and T98G cell lines showed an increase in ATP1B2. In addition to apoptosis induction of the U87 and T98G cell lines, ATP1B2 silencing induced GSC apoptosis, which indicates that ATP1B2 also plays important roles in GSCs. Theoretically, targeting both cancer cells and GSCs is a more promising and durable treatment to combating cancer [37].

Previous studies proved that Na^+/K^+-ATPase inhibition promotes sodium-calcium exchange and consequently elevates $[Ca^{2+}]i$ [38]. The calcium signal is an important second message, which has been implicated in a series of cellular events [39]. $[Ca^{2+}]i$ elevation plays an important role in apoptotic signaling [40]. The present study showed that downregulation of ATP1B2 increased the $[Ca^{2+}]i$ similar to digoxin treatment. Elevated Ca^{2+} levels have been reported following the activation of the MAPK pathway in certain cancer cells [41]. We demonstrated that ATP1B2 knockdown induced p38 kinase signaling pathway activation. Digoxin-treated GBM cell lines also showed robust phosphorylation of p38 at different times. Moreover, both ATP1B2 downregulation and digoxin treatment induced MMP loss and subsequently activated caspase-3. In this study, we demonstrated that the anti-GBM effect of ATP1B2 silencing was similar to that of digoxin *in vitro*. ATP1B2 knockdown also elevates $[Ca^{2+}]i$ similar to inhibition of Na^+/K^+-ATPase by cardiac glycosides in cancer cells [30]. These data indicate that ATP1B2 silencing tended to disrupt the Na^+/K^+-ATPase, which is similar to the actions of cardiac glycosides.

In conclusion, we examined the anticancer effects of ATP1B2 knockdown in GBM for the first time. Downregulation of ATP1B2 induced GBM cell apoptosis by increasing $[Ca^{2+}]i$ and activating p38 kinase. Furthermore, the low expression of ATP1B2 in heart muscles suggests that it might be a therapeutic target spe-

cifically for GBM to avoid cardiotoxicity. These results might also provide proof-of-concept evidence for the development of anticancer drugs targeting ATP1B2 in GBM therapies.

Disclosure of conflict of interest

None.

Abbreviations

GBM, glioblastoma; ATP1B2, ATPase Na^+/K^+ transporting subunit beta 2; GSCs, glioblastoma stem-like cells; $[Ca^{2+}]i$, intracellular Ca^{2+}; JC-1, 5,5',6,6'-tetrachloro-1,1',3,3'-tetraethyl-imidacarbocyanine iodide; BrdU, 5-Bromo-2'-deoxyuridin; EdU, 5-ethynyl-2'-deoxyuridine; DMEM, Dulbecco's modified Eagle's medium; EGF, epidermal growth factor; bFGF, basic fibroblast growth factor; dox, doxycycline; FITC, fluorescein isothiocyanate; PI, propidium iodide; qPCR, quantitative polymerase chain reaction; MAPK, mitogen-activated protein kinase; MMP, mitochondrial membrane potential.

Address correspondence to: Xudong Zhao, Key Laboratory of Animal Models and Human Disease Mechanisms of Chinese Academy of Sciences and Yunnan Province, Kunming Institute of Zoology, Chinese Academy of Sciences/Key Laboratory of Bioactive Peptides of Yunnan Province, 32 East Jiaochang Road, Kunming 650223, Yunnan, China. Tel: 1-86-871-68125430; E-mail: zhaoxudong@mail.kiz.ac.cn

References

[1] Jaitovich AA and Bertorello AM. Na+, K+-ATPase: an indispensable ion pumping-signaling mechanism across mammalian cell membranes. Semin Nephrol 2006; 26: 386-392.

[2] Xie ZJ and Askari A. Na+/K+-ATPase as a signal transducer. Eur J Biochem 2002; 269: 2434-9.

[3] Wang HJ, Haas M, Liang M, Cai T, Tian J, Li SW and Xie ZJ. Ouabain assembles signaling cas-

cades through the caveolar Na⁺/K⁺-ATPase. J Biol Chem 2004; 279: 17250-9.

[4] Rajasekaran SA, Huynh TP, Wolle DG, Espineda CE, Inge LJ, Skay A, Lassman C, Nicholas SB, Harper JF, Reeves AE, Ahmed MM, Leatherman JM, Mullin JM and Rajasekaran AK. Na, K-ATPase subunits as markers for epithelial-mesenchymal transition in cancer and fibrosis. Mol Cancer Ther 2010; 9: 1515-24.

[5] Mijatovic T, Roland I, Van Quaquebeke E, Nilsson B, Mathieu A, Van Vynckt F, Darro F, Blanco G, Facchini V and Kiss R. The alpha 1 subunit of the sodium pump could represent a novel target to combat non-small cell lung cancers. J Pathol 2007; 212: 170-9.

[6] Wang MW, Gu P, Zhang ZY, Zhu ZL, Geng Y, Kayed H, Zentgraf H and Sun XF. FXYD3 expression in gliomas and its clinicopathological significance. Oncol Res 2009; 18: 133-139.

[7] Lefranc F and Kiss R. The sodium pump alpha(1) subunit as a potential target to combat apoptosis-resistant glioblastomas. Neoplasia 2008; 10: 198-206.

[8] Wen PY and Reardon DA. Progress in glioma diagnosis, classification and treatment. Nat Rev Neurol 2016; 12: 69-70.

[9] Blanco G and Mercer RW. Isozymes of the Na-K-ATPase: heterogeneity in structure, diversity in function. Am J Physiol 1998; 275: F633-F650.

[10] Blanco G. Na, K-ATPase subunit heterogeneity as a mechanism for tissue-specific ion regulation. Semin Nephrol 2005; 25: 292-303.

[11] Platz EA, Yegnasubramanian S, Liu JO, Chong CR, Shim JS, Kenfield SA, Stampfer MJ, Willett WC, Giovannucci E and Nelson WG. A novel two-stage, transdisciplinary study identifies digoxin as a possible drug for prostate cancer treatment. Cancer Discov 2011; 1: 68-77.

[12] Schatzmann H. Herzglykoside als hemmstoffe für den aktiven Kalium-und Natriumtransport durch die Erythrocytenmembran. Helv Physiol Pharmacol Acta 1953; 11: 346-354.

[13] Woo A, James P and Lingrel J. Characterization of the fourth α isoform of the Na, K-ATPase. J Membr Biol 1999; 169: 39-44.

[14] Mekhail T, Kaur H, Ganapathi R, Budd GT, Elson P and Bukowski RM. Phase 1 trial of Anvirzel (TM) in patients with refractory solid tumors. Invest New Drugs 2006; 24: 423-427.

[15] Henary HA, Kurzrock R, Falchook GS, Naing A, Moulder SL, Wheler JJ, Tsimberidou AM, Durand J, Yang P, Johansen MJ, Newman R, Khan R, Patel U and Hong DS. Final results of a first-in-human phase I trial of PBI-05204, an inhibitor of AKT, FGF-2, NF-Kb, and p70S6K in advanced cancer patients. J Clin Oncol 2011; 29.

[16] Meng Z, Liu L, Shen Y, Yang P, Cohen L, Huo Y, Zhao Q, Ng C, Chang D and Garrett C. A randomized phase II study of gemcitabine (G) plus the cardiac glycoside huachansu (H) in the treatment of patients with locally advanced (LAPC) or metastatic pancreatic cancer (MPC). J Clin Oncol 2011; 29: 4127-4127.

[17] Bar EE, Lin A, Mahairaki V, Matsui W and Eberhart CG. Hypoxia increases the expression of stem-cell markers and promotes clonogenicity in glioblastoma neurospheres. Am J Pathol 2010; 177: 1491-1502.

[18] Badr CE, Wurdinger T, Nilsson J, Niers JM, Whalen M, Degterev A and Tannous BA. Lanatoside C sensitizes glioblastoma cells to tumor necrosis factor-related apoptosis-inducing ligand and induces an alternative cell death pathway. Neuro Oncol 2011; 13: 1213-1224.

[19] Aperia A. New roles for an old enzyme: Na, K-ATPase emerges as an interesting drug target. J Intern Med 2007; 261: 44-52.

[20] Adams KF, Gheorghiade M, Uretsky BF, Patterson JH, Schwartz TA and Young JB. Clinical benefits of low serum digoxin concentrations in heart failure. J Am Coll Cardiol 2002; 39: 946-953.

[21] Demiryürek A and Demiryürek S. Cardiotoxicity of digitalis glycosides: roles of autonomic pathways, autacoids and ion channels. Auton Autacoid Pharmacol 2005; 25: 35-52.

[22] Mijatovic T, Van Quaquebeke E, Delest B, Debeir O, Darro F and Kiss R. Cardiotonic steroids on the road to anti-cancer therapy. Biochim Biophys Acta 2007; 1776: 32-57.

[23] Mobasheri A, Avila J, Cozar-Castellano I, Brownleader MD, Trevan M, Francis MJO, Lamb JF and Martin-Vasallo P. Na⁺, K⁺-ATPase isozyme diversity; comparative biochemistry and physiological implications of novel functional interactions. Biosci Rep 2000; 20: 51-91.

[24] Antonicek H, Persohn E and Schachner M. Biochemical and functional-characterization of a novel neuron-glia adhesion molecule that is involved in neuronal migration. J Cell Biol 1987; 104: 1587-1595.

[25] Sun MZ, Kim JM, Oh MC, Safaee M, Kaur G, Clark AJ, Bloch O, Ivan ME, Kaur R, Oh T, Fouse SD, Phillips JJ, Berger MS and Parsa AT. Na(+)/K(+)-ATPase beta2-subunit (AMOG) expression abrogates invasion of glioblastoma-derived brain tumor-initiating cells. Neuro Oncol 2013; 15: 1518-1531.

[26] Geering K. The functional role of beta subunits in oligomeric P-type ATPases. J Bioenerg Biomembr 2001; 33: 425-438.

[27] Yu SC, Ping YF, Yi L, Zhou ZH, Chen HH, Yao XH, Gao L, Wang JM and Bian XW. Isolation and characterization of cancer stem cells from a human glioblastoma cell line U87. Cancer Lett 2008; 265: 124-134.

[28] Barwe SP, Anilkumar G, Moon SY, Zheng Y, Whitelegge JP, Rajasekaran SA and Rajasekaran AK. Novel role for Na, K-ATPase in phos-

phatidylinositol 3-kinase signaling and suppression of cell motility. Mol Biol Cell 2005; 16: 1082-1094.

[29] Rajasekaran SA, Palmer LG, Moon SY, Soler AP, Apodaca GL, Harper JF, Zheng Y and Rajasekaran AK. Na, K-ATPase activity is required for formation of tight junctions, desmosomes, and induction of polarity in epithelial cells. Mol Biol Cell 2001; 12: 3717-3732.

[30] McConkey DJ, Lin Y, Nutt LK, Ozel HZ and Newman RA. Cardiac glycosides stimulate Ca^{2+} increases and apoptosis in androgen-independent, metastatic human prostate adenocarcinoma cells. Cancer Res 2000; 60: 3807-3812.

[31] Hsu SS, Huang CJ, Cheng HH, Chou CT, Lee HY, Wang JL, Chen IS, Liu SI, Lu YC, Chang HT, Huang JK, Chen JS, Jan CR. Anandamide-induced Ca^{2+} elevation leading to p38 MAPK phosphorylation and subsequent cell death via apoptosis in human osteosarcoma cells. Toxicology 2007; 231: 21-29.

[32] Lefranc F, Mijatovic T, Kondo Y, Sauvage S, Roland I, Debeir O, Krstic D, Vasic V, Gailly P, Kondo S, Blanco G and Kiss R. Targeting the alpha 1 subunit of the sodium pump to combat glioblastoma cells. Neurosurgery 2008; 62: 211-221; discussion 221-212.

[33] Beguin P, Hasler U, Staub O and Geering K. Endoplasmic reticulum quality control of oligomeric membrane proteins: topogenic determinants involved in the degradation of the unassembled Na, K-ATPase alpha subunit and in its stabilization by beta subunit assembly. Mol Biol Cell 2000; 11: 1657-1672.

[34] Tokhtaeva E, Sachs G and Vagin O. Assembly with the Na, K-ATPase alpha(1) subunit is required for export of beta(1) and beta(2) subunits from the endoplasmic reticulum. Biochemistry 2009; 48: 11421-11431.

[35] Li L, Feng R, Xu Q, Zhang F, Liu T, Cao J and Fei S. Expression of the β3 subunit of Na^+/K^+-ATPase is increased in gastric cancer and regulates gastric cancer cell progression and prognosis via the PI3/AKT pathway. Oncotarget 2017; 8: 84285.

[36] Gloor S, Antonicek H, Sweadner KJ, Pagliusi S, Frank R, Moos M and Schachner M. The adhesion molecule on glia (Amog) is a homolog of the beta-subunit of the Na, K-Atpase. J Cell Biol 1990; 110: 165-174.

[37] Singh SK, Hawkins C, Clarke ID, Squire JA, Bayani J, Hide T, Henkelman RM, Cusimano MD and Dirks PB. Identification of human brain tumour initiating cells. Nature 2004; 432: 396-401.

[38] Aizman O, Uhlen P, Lal M, Brismar H and Aperia A. Ouabain, a steroid hormone that signals with slow calcium oscillations. Proc Natl Acad Sci U S A 2001; 98: 13420-13424.

[39] Berridge MJ, Lipp P and Bootman MD. The versatility and universality of calcium signalling. Nat Rev Mol Cell Biol 2000; 1: 11-21.

[40] Nicotera P and Orrenius S. The role of calcium in apoptosis. Cell Calcium 1998; 23: 173-180.

[41] Mu D, Zhang W, Chu D, Liu T, Xie Y, Fu E and Jin F. The role of calcium, P38 MAPK in dihydroartemisinin-induced apoptosis of lung cancer PC-14 cells. Cancer Chemother Pharmacol 2008; 61: 639-45.

Supplementary Table 1. qPCR primers used in the gene expression study

| Gene	Forward primer	Reverse primer
ATP1B2	GAGGACGCACCAGTTTATGGG	GGGGTATGGTCGGAGACAGT
Nestin	GCAGCAGGAAATATGGGAAG	TCTCATGGCTCTGGTTTTCC
SOX2	CAAGATGCACAACTCGGAGA	GCTTAGCCTCGTCGATGAAC
ATP1A1	AAAGGTGTGGGCATCATCTC	GCTTGCTTGGACACATCTGA
18S rRNA	GTAACCCGTTGAACCCCATT	CCATCCAATCGGTAGTAGCG

Supplementary Table 2. The target sequences of short hairpin RNA for ATP1B2

| shRNA	Target sequence
shATP1B2-1#	GAATGTAGAATGTCGCATCAA
shATP1B2-2#	GAACCTTGATGTCATTGTCAA
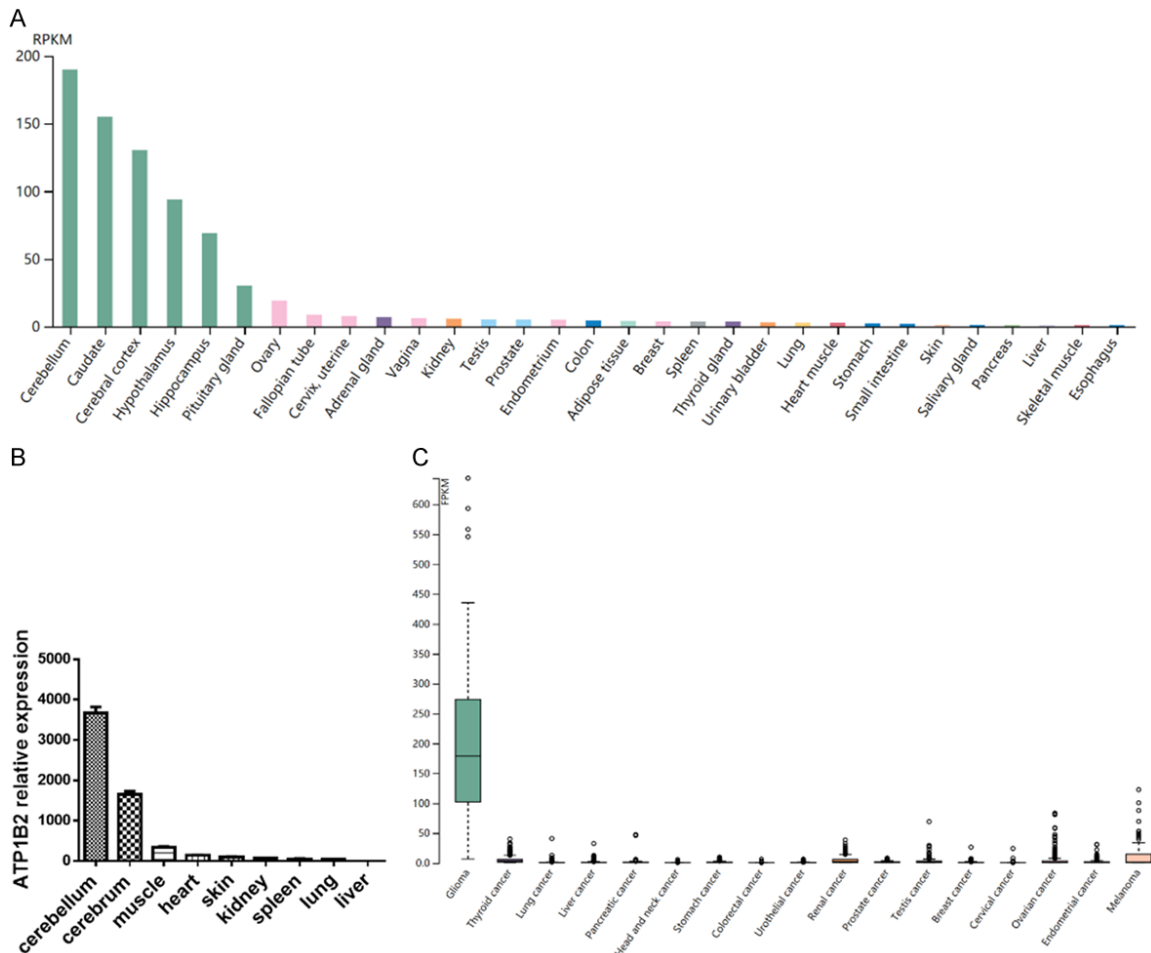
Supplementary Figure 1. ATP1B2 is expressed exclusively in human and mouse nervous system and GBM. A. ATP1B2 RNA expression levels from Human Protein Atlas (HPA). B. Quantitative polymerase chain reaction (qPCR) analysis of ATP1B2 expression levels in mouse tissues. ATP1B2 expression level was normalized to 18S rRNA. Data are means ± SD. C. RNA-seq data of ATP1B2 in 17 cancer types reported as median fragments per kilobase of exon per million reads (FPKM), generated by The Cancer Genome Atlas (TCGA).
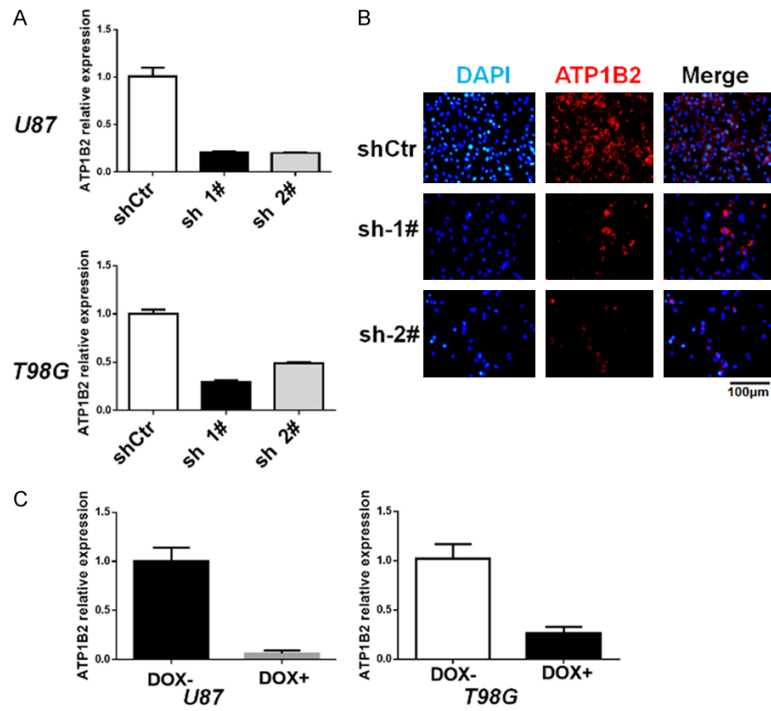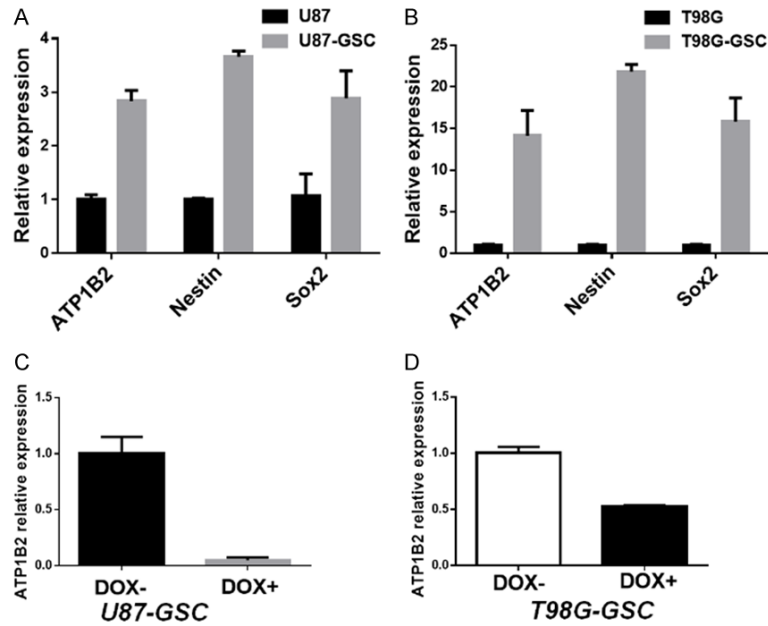
Supplementary Figure 2. Knockdown efficiency of ATP1B2 using short hairpin RNAs (shRNAs). (A, B) sh-1# and sh-2# knockdown efficiency in U87 and T98G cells using (A) qPCR and (B) immunofluorescence. (C) Doxycycline-inducible sh-1# knockdown efficiency in U87 and T98G by qPCR.
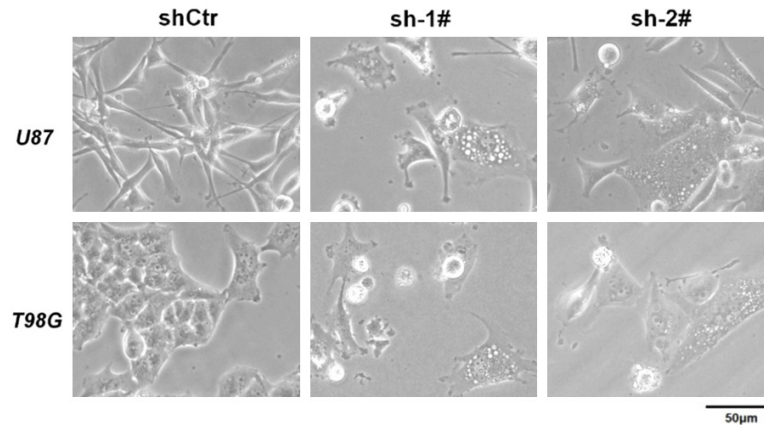

Supplementary Figure 3. The morphology of U87 and T98G cells after ATP1B2 was down-regulated.

Supplementary Figure 4. ATP1B2 and GSC markers are upregulated in GSCs and knockdown efficiency of ATP1B2 in GSCs. (A, B) Quantitative polymerase chain reaction (qPCR) analysis of ATP1B2 and GSC marker expression levels in (A) U87-GSC and (B) T98G-GSC cells. The expression level was normalized to 18S rRNA. Data are means ± SD. (C, D) Doxycycline-inducible shATP1B2-1# knockdown efficiency in (C) U87-GSC and (D) T98G-GSC using qPCR.
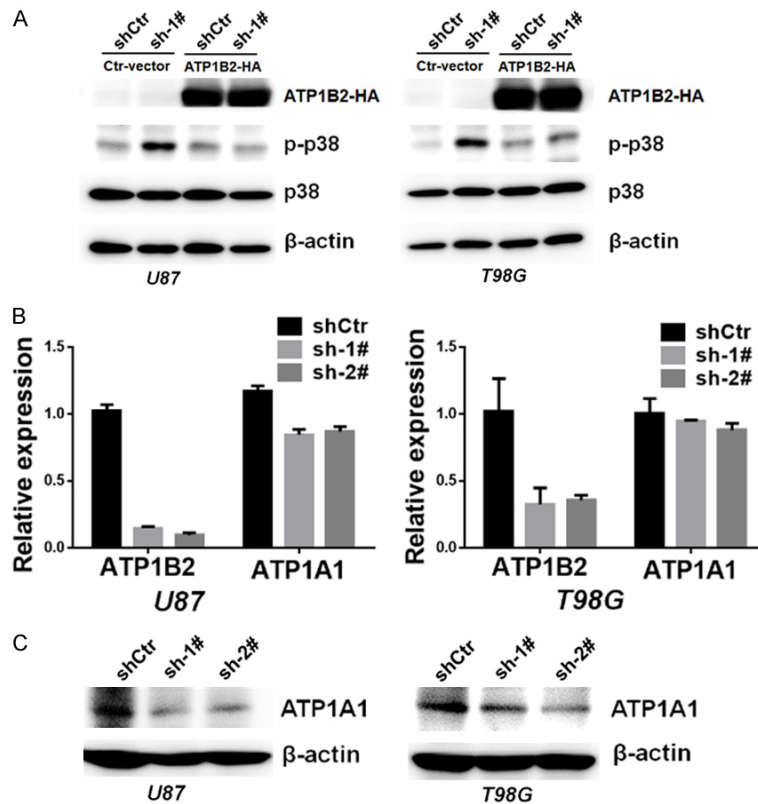
Supplementary Figure 5. ATP1B2 downregulation increases activates p38 mitogen-activated protein kinase (MAPK) pathway and decreases ATP1A1 expression. A. Downregulation of p38 activation in U87 and T98G cells with HA-tagged mutated human ATP1B2, which is not targeted for degradation by sh-1#. B. Quantitative PCR analysis of ATP1A1 expression after ATP1B2 downregulation in U87 and T98G cells. C. ATP1A1 expression were detected by western blotting using specific antibodies in U87 and T98G cells.